Photoluminescence polarization properties of single GaN nanowires containing $Al_xGa_{1-x}N/GaN$ quantum discs

L. Rigutti,[1,*] M. Tchernycheva,[1] A. De Luna Bugallo,[1] G. Jacopin,[1] F. H. Julien,[1] F. Furtmayr,[2] M. Stutzmann,[2] M. Eickhoff,[3] R. Songmuang,[4] and F. Fortuna[5]

[1]*Institut d'Electronique Fondamentale, University of Paris–Sud XI, UMR 8622 CNRS, 91405 Orsay, France*

[2]*Walter-Schottky-Institut, Technische Universität München, Am Coulombwall 3, 85748 Garching, Germany*

[3]*I. Physikalisches Institut, Justus-Liebig-Universität, Heinrich-Buff-Ring 16, 35392 Giessen, Germany*

[4]*CEA-CNRS Group "Nanophysique et Semiconducteurs," Institut Néel, 25 Rue des Martyrs, 38042/38054 Grenoble Cedex 9, France*

[5]*Centre de Spectroscopie Nucléaire et Spectroscopie de Masse, University of Paris–Sud XI, UMR 8609 CNRS, 91405 Orsay, France*

(Received 25 September 2009; revised manuscript received 4 December 2009; published 13 January 2010)

The polarization anisotropy of single GaN nanowires containing $Al_xGa_{1-x}N/GaN$ multiquantum disc (MQDisc) structures is characterized by polarization-resolved microphotoluminescence (μPL). Single nanowires exhibit at $T=4.2$ K two main luminescence contributions: one is peaked at $E=3.45-3.48$ eV related to near-band-edge GaN bulk excitonic transitions and is polarized parallel to the nanowire axis ($\boldsymbol{\pi}$ polarization) at moderate excitation-power density; the other, lying at higher energy, is related to excitonic transitions confined in the MQDisc and is polarized perpendicularly to the nanowire axis ($\boldsymbol{\sigma}$ polarization). The results are interpreted in terms of the selection rules for excitonic transitions in wurtzite semiconductor crystals and of the polarization anisotropy arising from the elongated nanowire shape. Finally, the analysis of photoluminescence at $T=300$ K shows that the thermal population of light-hole states in the MQDisc produces a blueshift of the PL peak when polarization is rotated from $\boldsymbol{\sigma}$ to $\boldsymbol{\pi}$.

DOI: 10.1103/PhysRevB.81.045411 PACS number(s): 78.40.Fy, 78.55.Cr

I. INTRODUCTION

With the development of semiconductor nanowire growth, the role of the geometrical shape of these nanoscale systems and its influence on the polarization anisotropy of optical absorption and emission spectra have been object of intense studies. Since the work on the polarized photodetection and photoluminescence of single InP nanowires by Wang *et al.*,[1] the interest for polarization properties of nanowire systems has extended to a wide variety of materials.[2–4]

The large dielectric index contrast between the nanowire and the surrounding medium, along with the cylindrical geometry of the nanowire, strongly favors absorption and emission of light with the electric field **E** polarized along the nanowire axis $\mathbf{c_w}$ ($\boldsymbol{\pi}$ polarization) compared to the light with electric field perpendicular to the nanowire axis ($\boldsymbol{\sigma}$ polarization).[1,5] The theoretical study by Ruda and Shik[6] has assessed that this is strictly valid in nanowires with a diameter d much smaller than both their height h and the light wavelength in the medium λ. The photoluminescence (PL) polarization can indeed oscillate from the direction parallel to perpendicular to the nanowire axis when the ratio d/λ increases.[7] Another source of polarization anisotropy stems from the fundamental properties of electronic states, which depend on the symmetry of the crystal lattice[8–10] and, for very thin nanowires ($d<10$ nm) on the nanowire diameter.[11,12] Even in bulk materials excitonic transitions are not, in general, isotropic. The cubic symmetry of zincblende (ZB) III-V binary compound semiconductors such as GaAs and InP allows for isotropic excitonic transitions but the situation radically changes in semiconductors with reduced symmetry such as the wurtzite (WZ) InP and GaN. The most striking difference regards the type A and B excitonic transitions (X_A and X_B), corresponding to a heavy hole (hh) (in the case of X_A) or light hole (lh) (in the case of X_B) bound to a conduction-band electron (hh-*e* and lh-*e*, respectively). In both ZB and WZ crystals the calculation of the dipole matrix elements for the X_A transition shows that this is forbidden in $\boldsymbol{\pi}$ polarization. However, the *hh* and *lh* bands are degenerate in the ZB structures, and the three axes *x*, *y*, and *z* are perfectly equivalent; therefore, the excitonic luminescence in the bulk is unpolarized. In WZ crystals there is a nonequivalent crystalline orientation *z* and the A and B bands are not degenerate. Therefore, the X_A emission in ideal WZ crystals is polarized in the *x*-*y* plane. The consequences of this anisotropy have been assessed in several works on binary homogeneous nanowires. The work by Schlager *et al.*,[13] in particular, assessed that PL spectra of binary GaN nanowires in $\boldsymbol{\pi}$ and $\boldsymbol{\sigma}$ polarizations corresponds to different excitonic contributions while Mishra *et al.*[14] evidenced that the PL of binary InP ZB (WZ) nanowires is $\boldsymbol{\pi}$ polarized ($\boldsymbol{\sigma}$ polarized).

In the case of nanowires containing heterostructures, the primary consequence of carrier confinement is the increase in the energy separation of hh and lh states. Consequently, the enhanced separation of the emission energies of the X_A and X_B excitons allows for probing a single type of exciton emission.

A limited number of theoretical[15] and experimental[5,16] works have been dedicated to the polarization properties of nanowire heterostructures, in particular, to $InAs_xP_{1-x}$ quantum dots (QD) in InP nanowires. The study by Niquet and Mojica[15] analyzed the polarization properties of the quantum-dot emission in terms of both wave-function symmetry and nanowire geometry, predicting an emission strongly $\boldsymbol{\sigma}$ polarized at $T=4.2$ K in InAs quantum dots with thickness $t_{dot}\leq 4$ nm. The experimental studies by

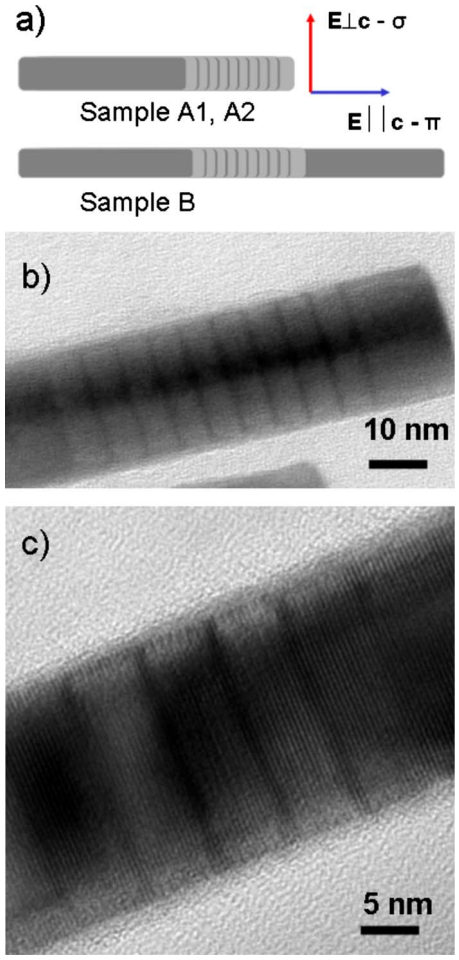

FIG. 1. (Color online) (a) Schematic representation of the analyzed nanowire samples A1, A2, and B. GaN and AlGaN regions are depicted in dark and light gray, respectively. (b) TEM image of one nanowire from sample A1, showing the multiquantum-disc region. (c) High-resolution TEM image of a nanowire from sample A2, showing the detail of atomic planes in the multiquantum-disc region.

Van Weert *et al.*,[5] performed on $InAs_{0.25}P_{0.75}$ with $t_{dot}=9$ nm embedded in InP nanowires, did not confirm the prediction. In this case, indeed, the quantum-dot PL polarization at $T=4.2$ K was found to be π type and imposed almost exclusively by the nanowire geometry.

Single and multiple quantum-disc structures (MQDisc) based on the $Al_xGa_{1-x}N/GaN$ material system have been extensively characterized.[17–21] However, no systematic study of the polarization properties of nanowires containing nitride-based quantum structures has been performed so far.

In this work we study the polarization-resolved microphotoluminescence (μPL) of GaN nanowires containing $Al_xGa_{1-x}N/GaN$ multiquantum discs. Three samples with different MQDisc parameters and doping concentrations have been investigated. All samples exhibit two main luminescence features: the near-band-edge (NBE) GaN emission and the quantum structure (MQDisc) emission, which allows investigating the polarization properties of both GaN and MQDisc excitonic luminescence within the *same* single wire. We demonstrate that at $T=4.2$ K the GaN luminescence, consisting of both X_A and X_B contributions, is π polarized as a consequence of the nanowire geometry and of the dielectric index contrast. However, at lower excitation-power densities the GaN luminescence is almost unpolarized because of the reduced contribution of the X_B recombination. In contrast, the MQDisc luminescence consists of only X_A contributions and is strongly σ polarized because of the selection rules for excitonic transitions within the investigated range of excitation power. Finally, the analysis of polarization properties was carried out at room temperature, where the thermally activated population of the X_B levels in the MQDisc system produces a blueshift of the MQDisc peak energy when rotating the polarization from σ to π.

TABLE I. Structural parameters of the analyzed nanowire samples.

	Sample A1	Sample A2	Sample B
Position of MQDisc system	Top	Top	Middle
Number of QDiscs	9	9	20
Disc thickness (nm)	1.5–1.75	1–1.25	1.5–2.5
Barrier thickness (nm)	5	5	2–3
Al x fraction in the barriers	5%	16%	100%
Nanowire height (nm)	400–450	400–450	1200–1300
Base height (nm)	350–400	350–400	~600
Cap height (nm)	20	20	~600
Al x fraction in the cap	5%	16%	0%
Nanowire diameter (nm)	25–50	25–50	25–40
Intentional doping	None	None	*n* type: Si

II. INVESTIGATED SAMPLES AND EXPERIMENTAL METHOD

The three nanowire samples containing quantum structures are schematically depicted in Fig. 1(a) and their parameters are listed in Table I. The catalyst-free GaN nanowires were grown by plasma-assisted molecular-beam epitaxy on Si(111) substrates at a substrate temperature of 780 °C. Nitrogen-rich conditions were employed in order to achieve self-assembled nanowire growth. Details on the growth technique can be found in Refs. 22 and 23.

A. Samples A1 and A2

The nanowires consist of a GaN base part (length approximately 350–400 nm), which is followed by a nine-period $Al_xGa_{1-x}N/GaN$ multiquantum-disc structure covered by a 20-nm-thick AlGaN cap with the same Al content as in the barriers. Sample A1 has a low Al content, $x=5\%$, while sample A2 has a higher Al content, $x=16\%$. The barrier thickness is $t_{barr}=5$ nm and the disc thickness is $t_{QD}=1-1.25$ nm ($t_{QD}=1.5-1.75$) nm for sample A1 (sample A2). Both the GaN base and the heterostructures are nominally undoped. Transmission electron microscopy (TEM) images of the heterostructure region of these samples are reported in Figs. 1(b) and 1(c). Well-defined QDiscs with thickness fluctuations on the order of a single monolayer (1

ML, corresponding to 0.26 nm in unstrained GaN) can be identified in the high-resolution TEM characterization of these structures.

B. Sample B

The heterostructure consists of a 20-period AlN/GaN MQDisc with structural parameters in the ranges $t_{barr}=2-3$ nm and $t_{QD}=1.5-2.5$ nm. The heterostructure was grown in the middle of a *n*-type doped GaN:Si nanowire, whose height is approximately $h=1.2$ μm.

C. Method

Single nanowires from each sample were detached by ultrasound bath from the Si substrates and dispersed in ethanol on Si/SiO_2 templates patterned by e-beam lithography. The surface density of nanowires is controlled by dispersion in the range $1-5\times10^6$ nanowires/cm^2, which is low enough to avoid simultaneous excitation of several wires with different orientations.

Micro-PL has been performed in the temperature range from 4.2–300 K. The samples were cooled down in a continuous-flow liquid He cryostat and excited by means of a frequency-doubled cw Ar^{++} ion laser at 244 nm. The laser was focused on the substrate surface in a spot with a diameter of ~3 μm by means of a UV microscope objective with 0.4 numerical aperture. The excitation power was set in the range 50 μW–1 mW except for the measurements of the dependence of the polarization ratio on the power density, for which the power was lowered down to 10 μW. The sample was imaged through a UV-sensitive camera in order to visualize the luminescence spot and to locate the nanowire. PL spectra were measured using a HR460 spectrometer with a 600 grooves/mm grating and a charge-coupled device camera. The energy resolution of the setup during these experiments was in the range of 1 meV. To analyze the emission polarization, a polarizer was placed at the entrance of the spectrometer. The response of the system to horizontally or vertically polarized light was calibrated using the UV light from different unpolarized sources with energies in the range 3.3–3.8 eV filtered by the polarizer at the spectrometer entrance. For each single nanowire analyzed by μPL, a series of spectra was taken at different values of the angle of the polarizer axis, which was varied over the whole interval $0°-360°$ with 30° step.

The orientation of the nanowire with respect to the polarizer axis, as well as its isolation from other dispersed nanowires, has been assessed by scanning electron microscopy measurements performed after the optical characterization. The lithographic patterning of the substrate served as a reference frame. We thus identified the polarizer angles closest to $\boldsymbol{\pi}$ and $\boldsymbol{\sigma}$ polarizations for each wire. For each PL peak the polarization ratio is defined as

$$P^{e}_{pk}=(I^{pk}_{\pi}-I^{pk}_{\sigma})/(I^{pk}_{\pi}+I^{pk}_{\sigma}), \quad (1)$$

where I^{pk}_{π} and I^{pk}_{σ} are the integrals of the PL intensity of the peak corresponding to the $\boldsymbol{\pi}$ and $\boldsymbol{\sigma}$ polarizations, respectively. When many excitonic contributions are significantly overlapped, as it occurs in the NBE PL of GaN, the integrals I^{pk}_{π} and I^{pk}_{σ} extend over the whole NBE band. The same analysis was carried out on several tenths of nanowires for statistical purposes. Different nanowires, even belonging to the same sample, can indeed show important differences in the spectral shape, which may arise from diameter and height dispersion, as well as from the effect of surface states induced by external contamination.

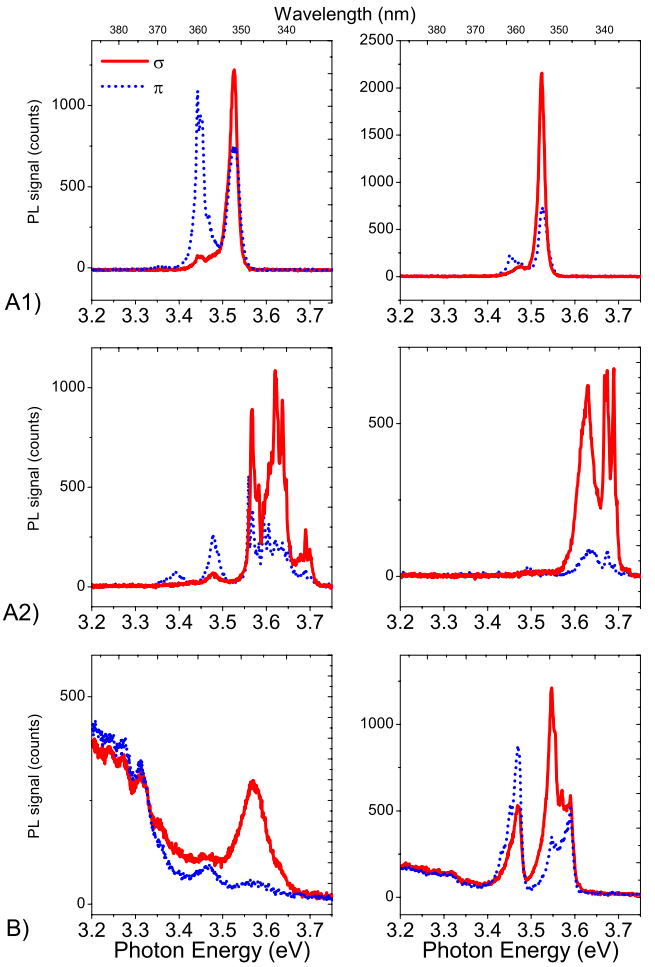

FIG. 2. (Color online) PL spectra at $\boldsymbol{\pi}$ (blue dotted lines) and $\boldsymbol{\sigma}$ polarization (red solid lines) collected from different individual nanowires belonging to the three samples described in Table I. First row refers to sample A1, second row refers to sample A2, and third row to sample B. All spectra were collected at temperature $T=4.2$ K.

III. LOW-TEMPERATURE PHOTOLUMINESCENCE

A. Spectral contributions

Typical micro-PL spectra of single nanowires from samples A1, A2, and B collected in $\boldsymbol{\pi}$ and $\boldsymbol{\sigma}$ configurations are reported in Fig. 2. All nanowire samples exhibit two main luminescence features: the one at 3.45–3.49 eV is attributed to the GaN NBE transitions in the bulk GaN region and the other one at higher energy is attributed to the Al(GaN)/GaN MQDisc excitonic transitions. The MQDisc

TABLE II. Emission energy E, average polarization ratio $\langle P^e \rangle$ and standard deviation of the polarization ratio ΔP^e of NBE and MQDisc PL in the analyzed nanowire samples.

		Sample A1	Sample A2	Sample B
NBE	E_{NBE} (eV)	3.45	3.47–3.48	3.47
	$\langle P^e_{NBE} \rangle$	0.77	0.48	0.39
	ΔP^e_{NBE}	0.14	0.13	0.12
MQDisc	E_{MQD} (eV)	3.53	3.55–3.72	3.55–3.65
	$\langle P^e_{MQD} \rangle$	−0.48	−0.7	−0.55
	ΔP^e_{MQD}	0.22	0.14	0.14

was chosen in order to exhibit fundamental transitions above the GaN bandgap (E_g=3.49 eV at 4.2 K). The typical energy values of the NBE and MQDisc luminescence are reported in Table II for the three samples. The luminescence peaks with energy lower than 3.42 eV, which are mostly found in sample B and are referred to as the subgap interval, can be related either to excitons bound to surface-defect states or to donor-acceptor pairs.[24] The contribution of donor-acceptor pairs is increased in intentionally doped samples such as sample B.[25]

1. GaN NBE luminescence

The NBE region corresponds to the luminescence of GaN originated by free excitons, or by excitons bound to donor states, to acceptor states and to point-defect states.[24–26] Micro-PL spectra from sample A1 nanowires are shown in Fig. 2A1. The GaN NBE emission is for most nanowires peaked at E_{NBE}=3.45 eV with a FWHM of 25 meV. It is ascribed to an exciton bound to a defect state, most likely located at the nanowire surface.[24,25,27] This contribution often masks the free and donor-bound excitons transitions expected at E=3.47–3.49 eV. These emission lines are however visible in the spectra of Fig. 2A1 although dominated by the defect-related peak.

Sample A2 nanowires [Fig. 2A2] exhibits a GaN NBE emission which is peaked at E_{NBE}=3.47–3.48 eV, ascribed to donor-bound exciton recombination, while the appearance of the peak at 3.45 eV is rare, in less than 10% of the analyzed single nanowires. This discrepancy with respect to the similar structures from sample A1 (differing by the heterostructure parameters) could be explained by slight growth parameter fluctuations, leading to a lower defect concentration in sample A2 nanowires.

In sample B [Fig. 2B] the NBE luminescence, depending on the investigated nanowire, appears either as a rather broadened peak at E_{NBE}=3.46–3.48 eV or as a structured peak in which donor-bound and free exciton contributions can be separated. The origin of the broadening is likely related to the intentional n-type doping and to the higher degree of strain induced by the lattice mismatch between AlN and GaN.

2. MQDisc luminescence

In sample A1 [Fig. 2A2] the MQDisc emission from single wires has a peak energy in the range E_{MQD} =3.518–3.534 eV, with a full width at half maximum (FWHM) of 12–16 meV. This peak is composed of the single emissions of each QDisc, which are not separately resolvable.

The MQDisc emission for sample A2 nanowires [Fig. 2A2] is represented by multiple narrow lines (FWHM in the range 10–2 meV) corresponding to the emission of single QDiscs with energies distributed in the range E_{MQD} =3.55–3.72 eV.

The MQDisc emission from sample B is peaked in the energy range E_{MQD}=3.55–3.6 eV. The emission FWHM is on the order of 35 meV 80% of the investigated nanowires [left-hand side spectrum of Fig. 2B]. Other nanowires show a multiple peak [right-hand side spectrum of Fig. 2B].

Effective-mass simulations have been carried out in order to assess the effect of the different thickness and of the different Al content in samples A1 and A2. The emission energies in sample A1 are less sensible to single-monolayer fluctuations. The QDisc PL energy predicted for sample A1 is $E^{5\%}_{7\ ML}$=3.54 eV for a QDisc thickness of 7 ML (1.75 nm) and $E^{5\%}_{6\ ML}$=3.55 eV for a QDisc thickness of 6 ML (1.5 nm). The same calculation for sample A2 yields a PL energy of $E^{16\%}_{4\ ML}$=3.69 eV for 4-ML- (1-nm)-thick QDiscs, and $E^{16\%}_{5\ ML}$=3.62 eV for 5-ML- (1.25-nm)-thick QDiscs. In both samples, the emission energies also depend on the position of the QDisc in the MQDisc structures. This is due to two main factors. The first factor is the axial band bending induced by the Fermi-level pinning on the polar top surface, which gives rise to a barrier height φ_b=1.2 eV.[18] The second factor is due to the relaxation effects of the strain accumulated at the GaN/AlGaN interface. The lattice constant relaxes rapidly to that of GaN in the direction of the GaN base and to that of AlGaN in the direction of the nanowire top. The typical decay length is on the order of the nanowire diameter.[28] Both the band bending and the strain relaxation result in a progressive blueshift of the PL energy from the GaN/AlGaN interface toward the top surface. However, the energy shift induced by these two mechanisms is quite different in the two samples. It can be estimated to be $\Delta E^{5\%}$=15 meV for sample A1 and $\Delta E^{16\%}$=35 meV for sample A2. This, together with the energy dispersion induced by possible monolayer fluctuations, accounts for the difference in the observed MQDisc spectral contributions in samples A1 and A2.

Similar considerations can be applied to the MQDisc luminescence of sample B, as effective-mass calculations for a MQDisc system with barrier and disc thickness t_{barr} =2.5 nm and t_{QD}=1.5–2.5 nm predict a PL energy in the range E=3.2–3.6 eV. The dispersion in the QDisc thickness in this structure is such to allow for PL luminescence under the GaN bandgap. However, the transitions in thicker discs yielding energies outside the range E=3.5–3.6 nm are strongly disfavored because of the weak superposition of the electron- and hole-envelope functions. In this sample, furthermore, the higher strain level induced by higher Al content, as well as the n-type Si doping introduce additional broadening mechanisms, which in most of the investigated nanowires yield spectra such as that reported in Fig. 2B on the left-hand side.

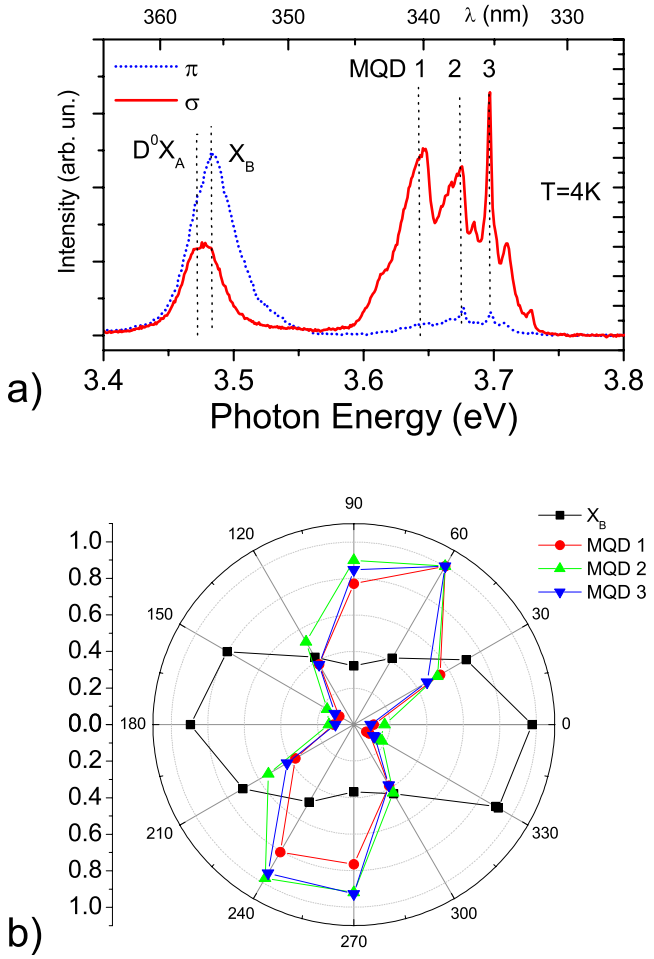

FIG. 3. (Color online) (a) Micro-PL (T=4.2 K) spectra from a single nanowire from sample A2 taken in $\boldsymbol{\pi}$ (blue dotted line) and in $\boldsymbol{\sigma}$ polarization (red solid line). (b) Normalized polar diagram illustrating the variation in the peak amplitudes according to the polarizer angle.

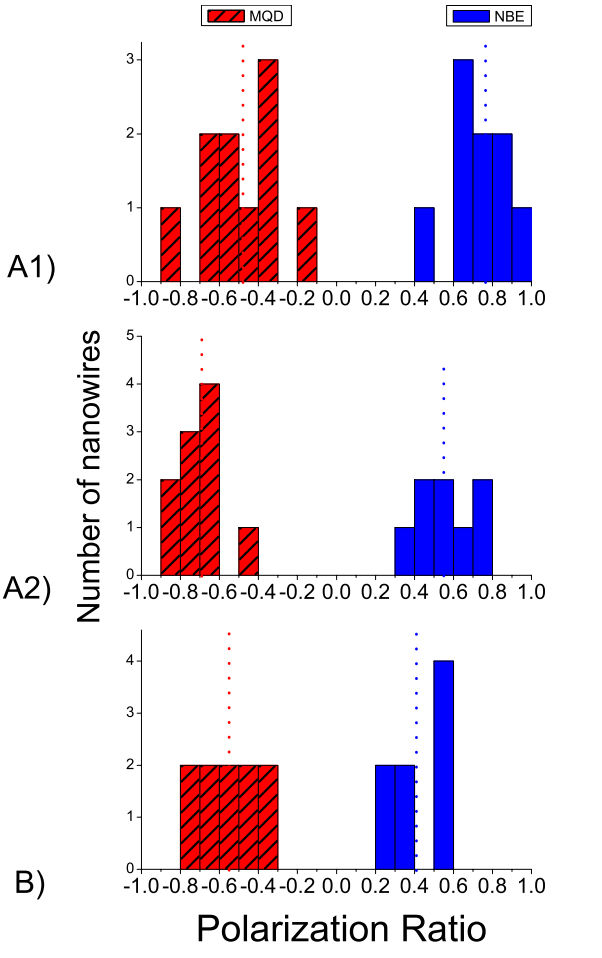

FIG. 4. (Color online) Statistics of the polarization ratio P^e for the different nanowire samples. Red-patterned and blue columns refer to the polarization degree of MQD and NBE luminescences, respectively. The dotted lines indicate the average values for the polarization degree of MQD and NBE for each sample. First plot refers to sample A1, second plot to sample A2, and third plot to sample B.

B. Polarization properties of NBE and MQDisc luminescence

Analyzing the polarization properties of the low-temperature PL spectra, we notice that in all nanowire samples the NBE luminescence is $\boldsymbol{\pi}$ polarized while the MQDisc luminescence is $\boldsymbol{\sigma}$ polarized. This result is independent of the number of quantum discs, of their position in the wire, and of the structural parameters of the quantum structure. This behavior is analyzed in more detail in Fig. 3, which presents the polarization-resolved μPL characterization of a sample A2 nanowire. Figure 3(a) shows the μPL spectra in $\boldsymbol{\pi}$ and $\boldsymbol{\sigma}$ configurations. Figure 3(b) reports the normalized intensities of the NBE peak and of the three major MQDisc peaks. For $\boldsymbol{\pi}$ polarization the intensity of the NBE component, peaked at E=3.48 eV in Fig. 3(a), is about twice that of the same component in $\boldsymbol{\sigma}$ polarization, which is peaked at 3.47 eV. The rotation from $\boldsymbol{\sigma}$ to $\boldsymbol{\pi}$ polarization thus produces both an intensity variation and a change in the spectral shape. The polar-intensity diagram in Fig. 3(b) corresponds to a typical dipole pattern. The NBE signal is $\boldsymbol{\pi}$ polarized with the polarization ratio P^e_{NBE}=0.34. In contrast, the MQDisc emission is $\boldsymbol{\sigma}$ polarized with the polarization ratio P^e_{MQD}=−0.86 for the peak labeled MQD-3 in the figure. Similar values are found for the peaks labeled MQD-1 and MQD-2. As a striking difference with the NBE case, the spectral shape of the MQDisc emission does not change from $\boldsymbol{\sigma}$ to $\boldsymbol{\pi}$ polarization, i.e., the energy position of the narrow peaks is independent of the angle.

The subgap luminescence is generally $\boldsymbol{\pi}$ polarized, following the same behavior as the NBE luminescence. This is visible for instance in the spectrum on the left-hand side of Fig. 2A2 for a defect-related emission at E=3.39 eV, or in the DAP emission present in the spectra of sample B, Fig. 2B.

A significant dispersion of the polarization ratios can be found within nanowires belonging to the same samples. The behavior of the ensemble of single nanowires has thus been analyzed in order to outline the peculiarities of each sample. The dispersion is reported for each sample in the histograms of Fig. 4. The average values and the standard deviations of the polarization ratios are reported in Table II. The number of analyzed single nanowires was on the order of 10 per sample.

As reported in Fig. 4A1, the polarization ratios for NBE and MQDisc emissions are $P^{e}_{NBE}=0.77\pm0.14$ and $P^{e}_{MQD}=-0.48\pm0.22$. In sample A2 [Fig. 4A2] the polarization ratio for the NBE luminescence is $P^{e}_{NBE}=0.55\pm0.13$ while for the MQDisc luminescence it is $P^{e}_{MQD}=-0.70\pm0.14$. It must be noted that in some nanowires from sample A2, such as in the one yielding the spectrum in the right-hand side of Fig. 2A2, MQDisc PL overwhelms NBE PL by nearly 2 orders of magnitude, showing that the relative intensity of NBE and MQDisc PL can significantly vary from wire to wire. This may be due to the dispersion in the surface-to-volume ratio which could affect the GaN emission efficiency but we cannot exclude that the effect is related to the position of the laser spot or to surface contamination. In sample B nanowires the polarization ratio for the NBE peak is $P^{e}_{NBE}=0.39\pm0.12$ while that for the MQDisc luminescence is $P^{e}_{MQD}=-0.55\pm0.14$.

The dispersion of polarization ratios is accounted for by two factors. The first factor is the imperfect alignment of the polarizer axis with the nanowire axis, which leads to a maximum error on the order of ±0.1. The second factor is the size dispersion of nanowires of the same sample. In any case, these results clearly show that NBE emissions are $\boldsymbol{\pi}$ polarized and all MQDisc emissions are $\boldsymbol{\sigma}$ polarized independently of the sample.

IV. DISCUSSION

A. Polarization of NBE luminescence

The statistics on the NBE emission of the analyzed nanowires was performed at moderate laser power density to obtain a good signal-to-noise ratio. This power level reveals sufficient to activate not only the fundamental X_A excitonic transition of GaN but also the X_B excitonic transition lying at higher energy. The NBE emission is composed of multiple contributions, allowed for both $\boldsymbol{\sigma}$ and $\boldsymbol{\pi}$ polarizations, with the exception of X_A, which is $\boldsymbol{\sigma}$ polarized. Indeed, in wurtzite crystal the selection rules for excitonic transitions are strongly anisotropic due to the reduced crystal symmetry and to the splitting of the hh and the lh bands. The dipole-matrix elements for excitonic transitions are defined as

$$M^{\mathrm{bulk},n}_{t,z}=|\langle u_c|p_{t,z}|u_{vn}\rangle|^2, \tag{2}$$

where $p_{t,z}$ indicates the component of the momentum operator perpendicular or parallel to the z axis (i.e., the [0001] crystallographic direction), respectively, $u_{c,vn}$ are the Bloch functions of the conduction band and of the nth valence band, respectively. The most important property states that excitonic transitions involving the heavy-hole level (hh-e, also denoted as exciton A, or X_A) are not allowed for the electric field polarization along the crystal z direction. Less strict selection rules apply for the transitions involving the light hole (lh-e, exciton B, or X_B) and the crystal-field split-off hole (ch-e, exciton C, or X_C).[9,10]

When the [0001] direction of the wurtzite crystal lattice corresponds to the nanowire axis $\mathbf{c_w}$, which is the case for the MBE-grown nanowires analyzed in this work, the luminescence peaks related to the X_A transitions (free and bound excitons) should be suppressed in the $\boldsymbol{\pi}$-polarized PL spectra. Observations of polarization anisotropy have been performed by Schlager *et al.*[13] in bulk GaN nanowires grown on the polar direction. The authors could assess the difference in the spectral shapes of $\boldsymbol{\sigma}$- and $\boldsymbol{\pi}$-polarized PL spectra of a pair of nanowires lying almost parallel on a Si substrate. A significant decrease in the X_A-related spectral component was observed in the $\boldsymbol{\pi}$-polarized spectrum. A more pronounced polarization contrast in the spectral shapes of $\boldsymbol{\pi}$- and $\boldsymbol{\sigma}$-polarized PL has been obtained by Paskov *et al.*[29] by analyzing the emission from free-standing polar GaN layers. However, a complete disappearance of the X_A-related lines in $\boldsymbol{\pi}$ configuration was not observed, which could be explained by the relaxation of the $\mathbf{k}\perp\mathbf{c}$ geometry caused by the rather high numerical aperture of the microscope objectives collecting the luminescence. The acceptance cone of the objective contains a significant amount of light with electric field having a nonzero component in the x-y plane. This explanation, put forward by Paskov *et al.* to explain the deviations from ideality of their spectra, can be applied to the case of nanowires as well.

However, due to the presence of the X_B and X_C lines in the NBE interval, the ensemble of the NBE luminescence can be roughly regarded as originated by an effective isotropically emitting dipole. Therefore, the polarization contrast of the NBE can be explained by the dielectric contrast theory, according to which X_B and X_C emissions and the resulting $\boldsymbol{\pi}$ polarization are favored. This is confirmed by the behavior of the NBE emission in Fig. 4. For $\boldsymbol{\pi}$ polarization the NBE component, peaked at $E=3.48$ eV, is about twice as intense as the same component in $\boldsymbol{\sigma}$ polarization, which is peaked at 3.47 eV. This energy shift supports the interpretation for a transition from a prevailing X_A character in the $\boldsymbol{\sigma}$ polarization to a prevailing X_B character in the $\boldsymbol{\pi}$ polarization, similarly to what is reported in the work by Schlager *et al.*[13] on homogeneous nanowires.

The polarization ratio observed in our experiment is somehow smaller than that reported in luminescence experiments on InP nanowires[1] and than the predictions by Ruda and Shik.[7] In the latter work, the polarization ratio P^{e} depends on the nanowire diameter d. For a value of the dielectric constant $\varepsilon/\varepsilon_0=9$ and under the hypothesis of isotropic dipole-matrix elements, P^{e} is expected to be larger than 0.7 for diameter values d smaller than 60 nm.[7] However, the internal dipole-matrix elements of the NBE emission cannot be considered isotropic because the dipole matrix element for the X_A exciton vanishes for the z direction. This contributes to the lower polarization contrast. It is also worth noting that the nanowires are not completely surrounded by vacuum, but lie on a Si/SiO_2 substrate, which lowers the effective dielectric index contrast, and, subsequently, the polarization contrast.

Concerning the peak centered at 3.45 eV, most authors agree that it can be assigned to an exciton bound to a defect[24,25,27] but very few is known on the exact nature of the defect, which might be of extended nature, and possibly located at the surface. As a partial conclusion, this study shows that the $\boldsymbol{\pi}$-type polarization tends to exclude a pure X_A character for this transition.

B. Polarization of MQDisc luminescence

As previously mentioned, the polarization behavior changes when the luminescence originated by MQDisc states is considered. The interpretation of this result is based on the effect of the confinement on the electronic levels. In a QDisc the X_A transition is energetically favored with respect to X_B as the quantum confinement produces an enhanced splitting of the energies of hh state and lh state. The magnitude of the splitting depends on the structural parameters defining the confining potential: the Al content in the AlGaN barriers, as well as the disc and barrier thickness. The role of the nanowire diameter can be neglected, as in most cases it largely exceeds the exciton Bohr radius, estimated as about 3 nm.[21] For this reason, the QDisc system can be described as a quantum well rather than as a quantum dot.

The dipole-matrix elements $M_{t,z}^{\mathrm{QW},n}$ for the excitonic transitions of states confined in a quantum well are given by[8]

$$M_{t,z}^{\mathrm{QW},n} = |\langle u_c|p_{t,z}|u_{vn}\rangle|^2|\langle \chi_c|\chi_{vn}\rangle|^2 = M_{t,z}^{\mathrm{bulk},n}|\langle \chi_c|\chi_{vn}\rangle|^2, \quad (3)$$

where $\chi_{c,vn}$ are the envelope functions of the conduction and of the nth valence-band states. Thus, the energetically favorable X_A transition in QDisc structures remains forbidden for $\boldsymbol{\pi}$ polarization. Considering the spectrum in Fig. 4(a), this behavior is the same for all the set of MQDisc lines, as underlined by the polar diagram in Fig. 4(b). The $\boldsymbol{\sigma}$ polarization of the MQDisc PL is a clear signature of the X_A character of this transition.

It is interesting to notice that the average polarization ratio for sample A1, $\langle P_{\mathrm{MQD}}^{\mathrm{e}}\rangle = -0.48$, is significantly weaker than that found for sample A2, $\langle P_{\mathrm{MQD}}^{\mathrm{e}}\rangle = -0.7$. The main difference between the two samples is the Al content, which is 5% for sample A1 and 16% for sample A2. The difference in Al fraction changes the PL emission energy and enhances the splitting ΔE_{AB} of the X_A and X_B energies from sample A1 to sample A2, which is most likely the reason of the increase in the polarization ratio in sample A2 nanowires. The splitting has been estimated by calculating the energy of hole levels in the framework of the effective-mass approximation for two $GaN/Al_xGa_{1-x}N$ quantum wells with GaN layer thickness $t_{\mathrm{QW}} = 1.5$ nm (1 nm), $Al_xGa_{1-x}N$ barrier thickness $t_{\mathrm{barr}} = 5$ nm, and Al fraction $x = 5\%$ ($x = 16\%$) corresponding to those of the QDiscs of sample A1 (A2), respectively. In the case of sample A1, $\Delta E_{\mathrm{AB}}^{5\%} = 12$ meV, while in the case of sample A2, $\Delta E_{\mathrm{AB}}^{16\%} = 25$ meV. It is worth pointing out that, the value for bulk GaN being $\Delta E_{\mathrm{AB}}^{\mathrm{bulk}} = 5$ meV,[29,30] carrier confinement significantly increases the energy-level splitting even for 5% Al content in the barrier.

The $\boldsymbol{\sigma}$ polarization of the MQDisc emission is independent of the QDisc position in the nanowire: it is $\boldsymbol{\sigma}$ polarized in samples A1 and A2, where the quantum structure is placed on top of the wire, and it is also $\boldsymbol{\sigma}$ polarized with a ratio $\langle P_{\mathrm{MQD}}^{\mathrm{e}}\rangle = -0.55$ in sample B, where the quantum structure is in the middle of the nanowire.

It should be noted that in the present system the influence of the nanowire elongated shape on the polarization of the MQDisc emission is strongly reduced. As the light emitted by the MQDisc system is above the GaN bandgap, this radiation is significantly absorbed in the GaN portion of the nanowire, leading to a decrease in the polarization anisotropy due to the dielectric contrast. This circumstance is different from the polarization-resolved experiments carried out by Zwiller *et al.*[16] on InAsP QD inside InP wires, which demonstrated that the QD emission is $\boldsymbol{\pi}$ polarized. The reason of the $\boldsymbol{\pi}$-type polarization observed by these authors could be accounted for by the theory of dielectric index contrast. First of all, the luminescence observed by Zwiller *et al.* has no pure X_A symmetry due to the significant quantum-dot thickness ($t_{\mathrm{dot}} \approx 9$ nm). Second, the QD luminescence is under the band gap of the InP and can therefore propagate along the nanowire.

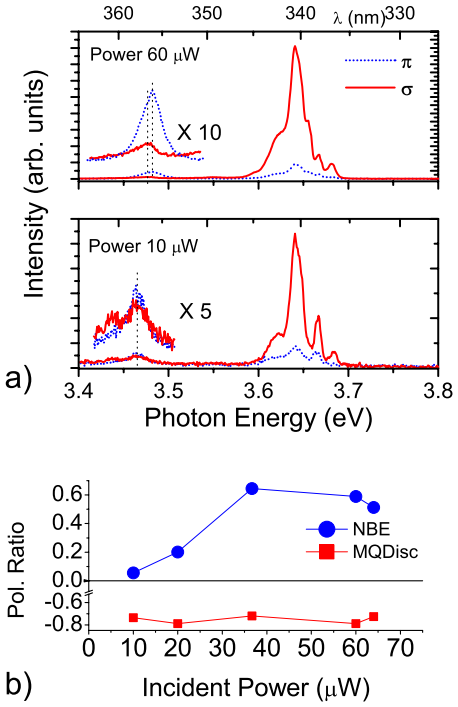

FIG. 5. (Color online) (a) $\boldsymbol{\pi}$-polarized (blue dotted line) and $\boldsymbol{\sigma}$-polarized (red solid line) micro-PL spectra ($T = 4.2$ K) from a single nanowire from sample A2 at different excitation powers. The NBE peak is expanded and vertically shifted for clarity. (b) The dependence of the polarization ratios of NBE and MQDisc emissions on the excitation power.

V. DEPENDENCE ON THE EXCITATION POWER

Polarization-resolved micro-PL was performed at $T = 4.2$ K at various laser-excitation powers. The spectra collected at 60 and 10 μW excitation powers are shown in Fig. 5(a). For 60 μW excitation power the polarization properties of the PL emission are similar to those reported in Fig. 3. The polarization ratios are $P_{\mathrm{MQD}}^{\mathrm{e}} = -0.78$ for MQDisc contribution and $P_{\mathrm{NBE}}^{\mathrm{e}} = 0.57$ for the NBE emission. The rotation of the polarization from $\boldsymbol{\sigma}$ to $\boldsymbol{\pi}$ induces a blueshift of the GaN NBE emission. When the excitation power is lowered down to 10 μW, the $P_{\mathrm{MQD}}^{\mathrm{e}}$ remains almost unchanged, while $P_{\mathrm{NBE}}^{\mathrm{e}}$ becomes close to zero. In contrast to high-excitation-power case, the peak energy of the NBE emission does not shift with the rotation of the polarization. The peak energy of the

low-power NBE emission is E_{NBE}=3.472 eV, close to the D^0X_A energy for both σ- and π-polarized spectra. Figure 5(b) summarizes the trend of both P^e_{NBE} and P^e_{MQD} with the excitation power. While P^e_{MQD} remains almost constant within the range of investigated power densities, P^e_{NBE} is close to zero for low-power levels, and increases at larger powers, up to 0.5–0.6. Similar values (0.48 ± 0.13) are measured for nanowires dispersed from sample A2.

The dependence of the NBE polarization ratio on the incident power can be interpreted as follows: at high excitation power, both X_A and X_B excitons participate to the radiative recombination. The effective radiating dipole can then be considered as quasi-isotropic and the polarization contrast is mostly determined by the dielectric contrast between the wire and the surrounding medium. At low excitation power, the contribution to the luminescence of X_B exciton is reduced. As a result, the polarization ratio of the NBE peak decreases with decreasing power. In the limit of a very low excitation power the polarization of NBE emission is expected to be determined exclusively by the X_A exciton polarization selection rules, i.e., it should be σ polarized with a negative value of the polarization ratio P^e_{NBE}. However, we did not observe the sign inversion of P^e_{NBE} due to the following reasons. The first reason is related to the setup and to the luminosity of the wire. The power level could not be decreased indefinitely because of the decreasing signal-to-noise ratio. Another factor relaxing the polarization contrast stems from the finite aperture of the objective, as discussed earlier. Furthermore, all NBE excitonic contributions in our samples are broadened, and a superposition of X_A and X_B energies is possible, leading to a certain relaxation of the selection rule itself.

VI. ROOM-TEMPERATURE PHOTOLUMINESCENCE

In order to further confirm our interpretation we have analyzed the effect of temperature on the polarization properties of nanowire systems. The complementary polarization of NBE and MQDisc PL is conserved as long as the energy difference between the X_A and X_B levels in the QDiscs is higher than the thermal energy $\Delta E_{AB} \gg k_B$ T. PL spectra collected at T=40 K and T=4.2 K show indeed the same behavior. When T is raised, the overall luminescence is quenched because of the thermally activated nonradiative recombination, which depopulates the exciton level X_A. At the same time, thermally activated carriers increase the population of the lh levels, giving rise to X_B photoluminescence,[31] which obeys to different selection rules than X_A, and is allowed for both σ and π polarizations.[9] In nanowire quantum structures, thermal population of higher-lying energy levels can lead to sign reversal of the polarization ratio.[15]

Due to the overall PL quenching, the characterization of *single* nanowires at room temperature is difficult, as the luminosity is too low to allow for an efficient location of the emitting wire. For this reason, we performed RT μPL characterization only on nanowire bundles, where all wires in a single bundle have the same spatial orientation. In these conditions, the theory of dielectric contrast is not strictly applicable to explain the observed polarization behavior. Indeed,

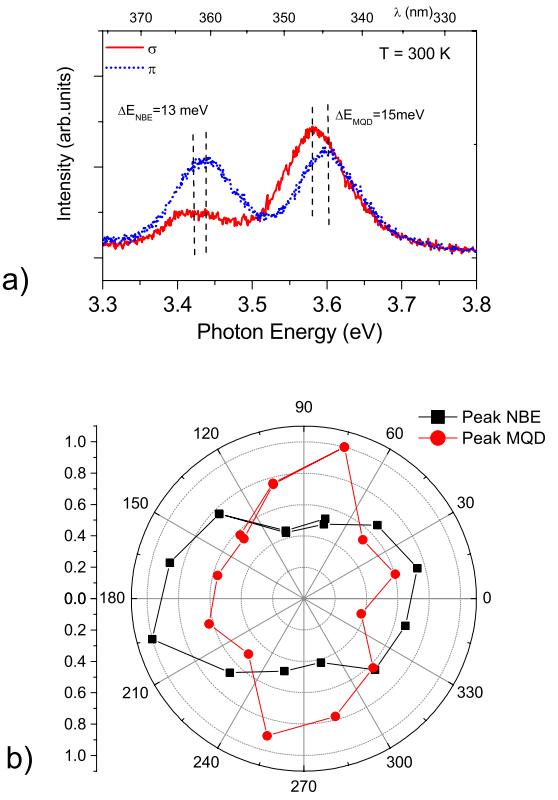

FIG. 6. (Color online) (a) Room temperature micro-PL spectra from a nanowire bundle from sample A2 taken in π (blue dotted line) and in σ polarization (red solid line). (b) Normalized polar diagram illustrating the variation in the peak amplitudes according to the polarizer angle.

the polarization of MQDisc PL is at RT different from wire to wire: it can have the same behavior as observed at T =4.2 K (σ polarization), be very weakly polarized, or even π polarized. In contrast, the NBE luminescence is in 80% of cases π polarized as at T=4.2 K. In Fig. 6(a) we report the RT μPL spectra taken in σ and π polarization of a nanowire bundle from sample A2. Both NBE and MQDisc emission peaks are thermally broadened, and the NBE peak is redshifted with respect to low temperature. No single narrow peaks can be resolved in the MQDisc emission. The polar diagram in Fig. 6(b) shows that the NBE PL is polarized along the nanowire axis. It also shows that the MQDisc PL is weakly σ polarized. Comparing the spectra taken at π and σ polarization, we notice that both NBE and MQDisc emissions blueshift when the polarization passes from σ to π. The NBE peak shifts by ΔE^{NBE}=13 meV while the MQDisc peak shifts by ΔE^{MQD}=15 meV. The same behavior was found in several other nanowire bundles. The average values for the shifts are $\langle \Delta E^{NBE} \rangle$=7 meV and $\langle \Delta E^{MQD} \rangle$=23 meV. These two quantities should be considered as an estimation of the separation energy between X_A and X_B excitons, whose value as already mentioned is ΔE^{NBE}_{AB}=5 meV in bulk GaN (Refs. 29–31) and $\Delta E^{16\%}_{AB}$=25 meV in QDiscs such as those contained in sample A2 nanowires. The good agreement between the blueshifts and the estimation of the separation energy between X_A and X_B represents thus a confirmation of our interpretation of polarization-resolved PL.

VII. CONCLUSIONS

In this work we reported the results obtained from an extensive polarization-resolved microphotoluminescence study on different samples of GaN nanowires containing $Al_xGa_{1-x}N/GaN$ multiquantum-disc systems. We investigated the low-temperature polarization properties of both binary GaN and MQDisc excitonic luminescence within the same single wire, for a statistically representative ensemble of wires. In particular, we were able to assess that the low-temperature GaN near-band-edge luminescence is $\boldsymbol{\pi}$ polarized as a consequence of the nanowire geometry and of the dielectric index contrast between the wire and the surrounding medium. The MQDisc low-temperature luminescence is strongly $\boldsymbol{\sigma}$ polarized as according to the selection rules for the dipole-matrix elements, which become more easily accessible because of the confinement-induced splitting of the X_A and X_B transition energies. The room-temperature polarization behavior of NBE and MQDisc emission is strongly influenced by the thermally induced population of X_B levels which is directly observed as a blueshift of the PL peaks from the X_A energy, observed in $\boldsymbol{\sigma}$ polarization, to the X_B energy observed in $\boldsymbol{\pi}$ polarization.

In conclusion, by analyzing the polarization of the MQDisc emission we provided an experimental proof of its pure X_A character at low temperature and an estimation of the energy separation between the X_A and X_B confined levels at room temperature. These nanowires represent a nanoscale system in which the two main luminescence contributions are mutually perpendicularly polarized, a peculiarity which could be exploited for nanophotonics applications.

ACKNOWLEDGMENTS

This work was supported in part by the French ANR agency under the Programs No. ANR-08-NANO-031 BoNaFo and No. ANR-08-BLAN-0179 NanoPhotoNit. The authors from J.L.U. and W.S.I. acknowledge financial support from the European Commission with the project DOTSENSE (Grant No. STREP 224212).

*Author to whom correspondence should be addressed; lorenzo.rigutti@ief.u-psud.fr

[1] J. Wang, M. S. Gudiksen, X. Duan, Y. Cui, and C. M. Lieber, Science **293**, 1455 (2001).
[2] S. Han, W. Jin, D. Zhang, T. Tang, C. Li, X. Liu, Z. Liu, B. Lei, and C. Zhou, Chem. Phys. Lett. **389**, 176 (2004).
[3] Y. Yu, V. Protasenko, D. Jena, H. Xing, and M. Kuno, Nano Lett. **8**, 1352 (2008).
[4] H.-Y. Li, S. Rühle, R. Khedoe, A. F. Koenderink, and D. Vanmaekelbergh, Nano Lett. **9**, 3515 (2009).
[5] M. H. M. van Weert, N. Akopian, U. Perinetti, M. P. van Kouwen, R. E. Algra, M. A. Verheijen, E. P. A. M. Bakkers, L. P. Kouwenhoven, and V. Zwiller, Nano Lett. **9**, 1989 (2009).
[6] H. E. Ruda and A. Shik, Phys. Rev. B **72**, 115308 (2005).
[7] H. E. Ruda and A. Shik, J. Appl. Phys. **100**, 024314 (2006).
[8] G. Bastard, *Wave Mechanics Applied to Semiconductor Heterostructures* (Les Editions de la Physique, Paris, 1990).
[9] S. L. Chuang and C. S. Chang, Phys. Rev. B **54**, 2491 (1996).
[10] M. Kumagai, S. L. Chuang, and H. Ando, Phys. Rev. B **57**, 15303 (1998).
[11] A. V. Maslov and C. Z. Ning, Phys. Rev. B **72**, 125319 (2005).
[12] M. P. Persson and A. Di Carlo, J. Appl. Phys. **104**, 073718 (2008).
[13] J. B. Schlager, N. A. Sanford, K. A. Bertness, J. M. Barker, A. Roshko, and P. T. Blanchard, Appl. Phys. Lett. **88**, 213106 (2006).
[14] A. Mishra, L. V. Titova, T. B. Hoang, H. E. Jackson, L. M. Smith, J. M. Yarrison-Rice, Y. Kim, H. J. Joyce, Q. Gao, H. H. Tan, and C. Jagadish, Appl. Phys. Lett. **91**, 263104 (2007).
[15] Y.-M. Niquet and D. Camacho Mojica, Phys. Rev. B **77**, 115316 (2008).
[16] V. Zwiller, N. Akopian, M. van Weert, M. van Kouwen, U. Perinetti, L. Kouwenhoven, R. Algra, J. Gomez Rivas, E. Bakkers, G. Patriarche, L. Liu, J.-C. Harmand, Y. Kobayashi, and J. Motohisa, C. R. Phys. **9**, 804 (2008).
[17] J. Ristić, E. Calleja, M. A. Sanchez-Garcia, J. M. Ulloa, J. Sanchez-Paramo, J. M. Calleja, U. Jahn, A. Trampert, and K. H. Ploog, Phys. Rev. B **68**, 125305 (2003).
[18] J. Ristić, C. Rivera, E. Calleja, S. Fernandez-Garrido, M. Povoloskyi, and A. Di Carlo, Phys. Rev. B **72**, 085330 (2005).
[19] U. Jahn, J. Ristić, and E. Calleja, Appl. Phys. Lett. **90**, 161117 (2007).
[20] M. Tchernycheva, C. Sartel, G. Cirlin, L. Travers, G. Patriarche, J.-C. Harmand, Le Si Dang, J. Renard, B. Gayral, L. Nevou, and F. Julien, Nanotechnology **18**, 385306 (2007).
[21] J. Renard, R. Songmuang, C. Bougerol, B. Daudin, and B. Gayral, Nano Lett. **8**, 2092 (2008).
[22] F. Furtmayr, M. Vielemeyer, M. Stutzmann, J. Arbiol, S. Estradé, F. Peirò, J. R. Morante, and M. Eickhoff, J. Appl. Phys. **104**, 034309 (2008).
[23] R. Songmuang, O. Landre, and B. Daudin, Appl. Phys. Lett. **91**, 251902 (2007).
[24] L. H. Robins, K. A. Bertness, J. M. Barker, N. A. Sanford, and John B. Schlager, J. Appl. Phys. **101**, 113506 (2007).
[25] F. Furtmayr, M. Vielemeyer, M. Stutzmann, A. Laufer, B. K. Meyer, and M. Eickhoff, J. Appl. Phys. **104**, 074309 (2008).
[26] L. H. Robins, K. A. Bertness, J. M. Barker, N. A. Sanford, and J. B. Schlager, J. Appl. Phys. **101**, 113505 (2007).
[27] M. A. Reshchikov and H. Morkoç, J. Appl. Phys. **97**, 061301 (2005).
[28] F. Glas, Phys Rev. B **74**, 121302 (2006).
[29] P. P. Paskov, T. Paskova, P. O. Holtz, and B. Monemar, Phys. Rev. B **70**, 035210 (2004).
[30] A. Wysmolek, K. P. Korona, R. Stepniewski, J. M. Baranowski, J. Bloniarz, M. Potemski, R. L. Jones, D. C. Look, J. Kuhl, S. S. Park, and S. K. Lee, Phys. Rev. B **66**, 245317 (2002).
[31] M. Leroux, N. Grandjean, B. Beaumont, G. Nataf, F. Semond, J. Massies, and P. Gibart, J. Appl. Phys. **86**, 3721 (1999).